Exp Astron (2005) 20:405–412
DOI 10.1007/s10686-006-9068-8

ORIGINAL ARTICLE

The MPE X-ray test facility PANTER: Calibration of hard X-ray (15–50 kev) optics

M. J. Freyberg · H. Bräuninger · W. Burkert · G. D. Hartner · O. Citterio · F. Mazzoleni · G. Pareschi · D. Spiga · S. Romaine · P. Gorenstein · B. D. Ramsey

Received: 13 February 2006 / Accepted: 26 July 2006

Abstract The Max-Planck-Institut für extraterrestrische Physik (MPE) in Garching, Germany, uses its large X-ray beam line facility PANTER for testing X-ray astronomical instrumentation. A number of telescopes, gratings, filters, and detectors, e.g. for astronomical satellite missions like *Exosat*, *ROSAT*, *Chandra (LETG)*, *BeppoSAX*, *SOHO (CDS)*, *XMM-Newton*, *ABRIXAS*, *Swift (XRT)*, have been successfully calibrated in the soft X-ray energy range (<15keV). Moreover, measurements with mirror test samples for new missions like *ROSITA* and *XEUS* have been carried out at PANTER. Here we report on an extension of the energy range, enabling calibrations of hard X-ray optics over the energy range 15–50 keV. Several future X-ray astronomy missions (e.g., *Simbol-X*, *Constellation-X*, *XEUS*) have been proposed, which make use of hard X-ray optics based on multilayer coatings. Such optics are currently being developed by the Osservatorio Astronomico di Brera (OAB), Milano, Italy, and the Harvard-Smithsonian Center for Astrophysics (CfA), Cambridge, MA, USA. These optics have been tested at the PANTER facility with a broad energy band beam (up to 50 keV) using the *XMM-Newton* EPIC-pn flight spare CCD camera with its good intrinsic energy resolution, and also with monochromatic X-rays between C-K (0.277 keV) and Cu-Kα (8.04 keV).

Keywords X-ray astronomy · X-ray telescopes · X-ray optics · X-ray detectors · Multilayers · Calibration
PACS: 95.55.Ka, 95.55.Aq, 41 50.+h, 07.85.Fv

M. J. Freyberg (✉) · H. Bräuninger · W. Burkert · G. D. Hartner
Max-Planck-Institut für extraterrestrische Physik, PANTER X-ray Test Facility, Gautinger Straße 45, 82061 Neuried, Germany
e-mail: mjf@mpe.mpg.de

O. Citterio · F. Mazzoleni · G. Pareschi · D. Spiga
INAF–Osservatorio Astronomico di Brera, Via Bianchi 46, 23807 Merate (lc), Italy

S. Romaine · P. Gorenstein
Harvard-Smithsonian Center for Astrophysics, Cambridge, MA 02138, USA

B. D. Ramsey
Space Science Department, NASA/MSFC, Huntsville, AL 35812, USA

1 Introduction

Until 1962 the Sun was the only known extraterrestrial X-ray source. A ballistic rocket flight equipped with a Geiger-Müller counter revealed the existence of a distant bright X-ray source (Sco X-1) and of an unresolved apparently diffuse emission [1]. Then, X-ray astronomy was soon recognised as an important way to study the high energy universe. Enormous progress in instrumentation for X-ray astronomical satellite missions has been made since these early days. The *ROSAT* mission was a milestone with the first imaging *All-Sky Survey* in the soft X-ray energy band (0.08–2.4 keV). This became possible by using a low-background position-sensitive detector combined with a high-throughput X-ray mirror system [2]. To develop and characterise the *ROSAT* optics the PANTER X-ray test facility was built (for reviews on X-ray telescopes and instrumentation see [3] and [4]).

Wolter showed that a combination of paraboloid and hyperboloid surfaces under grazing incidence can be used as an imaging X-ray optics system [5, 6]. The reflectivity of X-rays decreases rapidly with increasing incidence angle. With nested confocal and coaxial mirrors the total reflecting area can be increased (Figure 1), the inner shells contribute most of the area at higher energies while at lower energies the outer shells (with larger incidence angles) are significant. The so-called *Wolter-I geometry* is now a standard arrangement for astronomical X-ray telescopes. As an example: one *XMM-Newton* X-ray mirror module [7] is made of 58 gold-coated thin nickel (electroforming replication) shells with a maximum diameter of about 70 cm, focal length 7500 mm, and a total effective area of 1475 cm^2 at 1 keV. Another example is the *Chandra* thick polished mirror shells with an excellent on-axis point spread function of $\leq$1". A conic approximation to the paraboloid-hyperboloid geometry is realized by the *Astro-E2* thin foil mirrors which are very light-weight, but at the price of reduced spatial resolution. Several future X-ray astronomy missions (e.g., *Simbol-X* and *Constellation-X*) have been proposed which carry hard X-ray optics based on multilayer

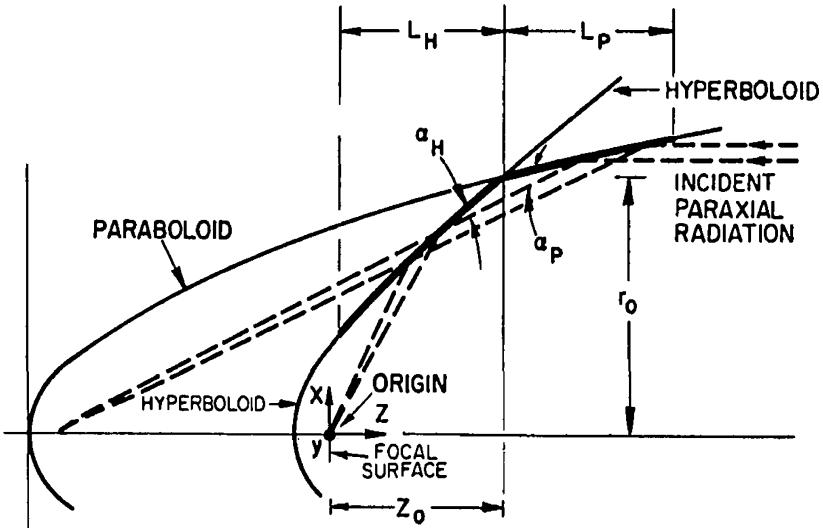

Fig. 1 Grazing incidence X-ray telescope principle in Wolter-I geometry (paraboloid and hyperboloid), illustration taken from [6]. For a parallel input beam the grazing incidence angles at paraboloid (α_p) and hyperboloid (α_h) are identical; for a finite source distance (divergent beam) α_p increases while α_h decreases, leading to an image distance greater than the focal length

coatings. With numerous stacks of alternating layers of low and high atomic number (e.g., W/Si, Pt/C) with different thicknesses (from about 1 nm to 10 nm) a significant increase of reflectivity at high energies (10–80 keV) on the basis of Bragg reflection (constructive interference) can be achieved [8, 9].

2 The MPE X-ray test facility PANTER

2.1 Overview

The imaging performance of optics is ideally characterised by parallel illumination, both on- and off-axis. On ground the realization of a wide aperture parallel X-ray beam is difficult. The simplest approximation of a parallel beam is placing a point-like X-ray source at the largest possible distance, thereby minimising the divergence of the beam with respect to the aperture size of the optics to be tested. Another approach – giving up full illumination of the mirror system – is via pencil beams, where the aperture of the incident X-ray beam is very small and the beam can thus be assumed to be parallel. This, however, increases measurement times tremendously.

In the case of the PANTER facility the distance from the X-ray sources (see Section 2.2) to the entrance of the instrument chamber is 123.6 m (Figure 2) [10]. The experiments (mirrors, gratings, filters, etc.) are placed in this 12.5 m long and 3.5 m diameter chamber. They can be moved and rotated by means of manipulators driven by stepper motors with a typical accuracy of $<3\,\mu$m. The X-ray source, tube, and chamber are kept under high vacuum at a pressure of $\leq 10^{-6}$ mbar. Two cryo-pumps (with a pumping capacity of $160\,\mathrm{m^3\,s^{-1}}$ each) reduce the partial pressure of water vapour in the chamber by a factor of 10 or more, to avoid icing on the cooled CCD camera (see Section 2.3). Valves, pumps, manipulators, detectors, X-ray sources, etc., can be remotely controlled from the control room. All relevant parameters of the facility are logged and can be used in later analysis. The cleanliness of the facility is measured continuously; the chamber and the preparation room are temperature-stabilised clean areas of class 1000.

2.2 X-ray sources

For calibration at the PANTER facility four different X-ray sources are available. These X-ray sources are mounted on a rail system and the exchange is done within a couple of hours.

The main source is an open X-ray source using a target wheel with 16 different targets which provide characteristic X-ray lines of the target element between 0.28 keV (C-K) and 12 keV (Au-L). This source is accompanied by two filter wheels to suppress selected parts of the

Fig. 2 Overview of the X-ray Test Facility PANTER situated in Neuried in the southwest of Munich, with a 123 m vacuum tube connecting the X-ray sources (located to the right) and the instrument chamber (on the left of the image)

spectrum, e.g., the continuum or Kβ lines. A target change can be performed within minutes. Fluxes are of the order of 1–10 $\times 10^3$ photons cm^{-2} s^{-1}, depending slightly on the material and filters chosen. For very high fluxes and energies a commercial (sealed) X-ray source is available which provides a couple of X-ray lines in the 4.5–22 keV range and bremsstrahlung continuum up to 50 keV.

Moreover, two tunable monochromators can be used to study the performance of X-ray optics in the vicinity of the relevant X-ray absorption edges. The reflection grating monochromator covers the softer energy band (0.25–1.0 keV, up to 2 keV using second order), while the double crystal monochromator provides photon energies between 1.5–25 keV (incl. second order). The energy resolution of each system is better than 4% (and much better in cross-dispersion direction).

2.3 Focal plane instrumentation

The flight spare models of the *ROSAT* Position Sensitive Proportional Counter (PSPC) and the *XMM-Newton* EPIC-pn CCD camera serve as focal plane X-ray detectors for calibration measurements. The PSPC [11, 12] provides moderate spectral (40% at 0.93 keV) and spatial (280 μm) resolution, but it is well-suited for measuring effective areas as it is an exact photon counting device and not, for example, affected by pile-up (two photons hitting the same or neighbouring pixels in the same read-out cycle) present in CCD devices when exposed to high fluxes. The PSPC wide field-of-view of 80 mm diameter is useful for alignment procedures as well as for the analysis of mirror scattering.

The EPIC-pn CCD camera [13] is used if higher spatial (150 μm pixels) or spectral (150 eV at 6 keV) resolution is required. It consists of 12 CCDs with 64 $\times$ 200 pixels on a monolithic silicon wafer with an area of about 6 $\times$ 6 cm^2. As a backside-illuminated device it is intrinsically radiation hard. It is operated at -90° C. The quantum efficiency (QE) is high throughout the energy band (Figure 3), even at 30 keV the QE exceeds 8%. The camera can be operated in various read-out modes, with the *Full-Frame* (FF) and *Small-Window* (SW) modes being the most relevant ones for our report. In FF mode the full CCD area is readout with a cycle time of 73.36 ms. In SW mode only an area of 64 $\times$ 64 pixels in one CCD is read out, allowing a shorter cycle time of only 5.67 ms which significantly reduces pile-up effects. Moreover, the camera can be operated with two different gains, the high-gain mode with an energy range of 0.1–17 keV, and a low-gain mode with a factor of about 18 higher energies.

It is planned to use the new frame-store CCD devices [14] developed for ROSITA [15] for a new camera at the PANTER facility. This camera will have smaller pixel size, better energy resolution, and increased thickness (and thus high-energy QE) and represents one aspect of a "growing facility". The improved spatial resolution of the new camera will also be important for measurements of mirror test samples for missions like *XEUS* [16].

3 Multi-layer mirror calibration

As already mentioned above, a finite source distance d changes the performance parameters such as the location of the image to $z = f \times d/(d - f)$ instead of f, where f denotes the focal length, and also the incidence angles on the paraboloid and hyperboloid (Figure 1). An increased grazing incidence angle at the paraboloid means a reduction in reflectivity, which is not fully compensated by the decreased hyperboloid incidence angle. With the additional

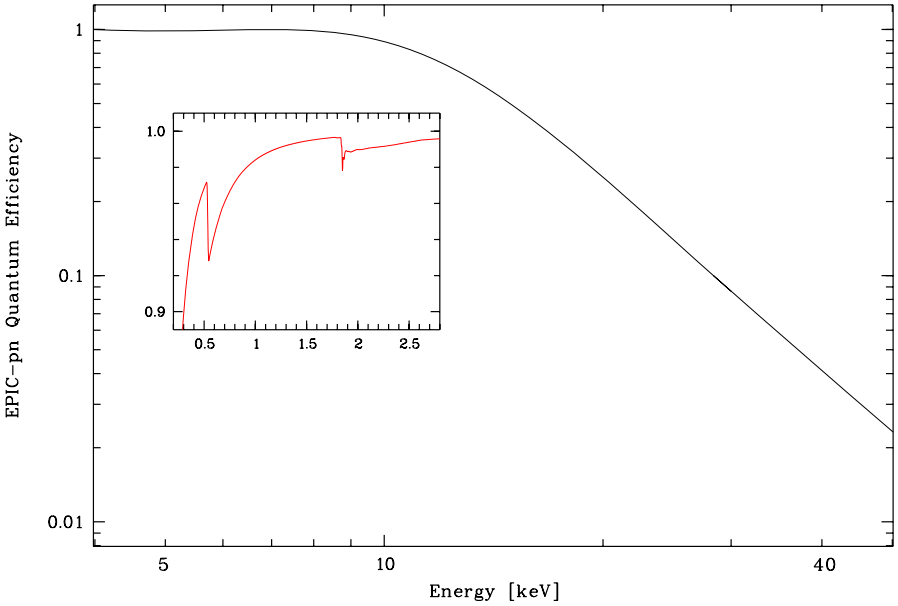

Fig. 3 Quantum efficiency (QE) of the *XMM-Newton* EPIC-pn CCD camera as function of energy from 4–50 keV. The insert shows the range 0.2–2.8 keV and the effects of oxygen and silicon edges. Above 8 keV the efficiency is dominated by the absorption probability in the 300 μm bulk of silicon, at 30 keV the QE is about 8.7% (2.3% and 0.7% at 50 keV and 80 keV, respectively)

Fig. 4 Spider module holding one multilayer coated mirror shell (at the ring), the shutter door is seen at the right of the module, the hole in the centre is used for flat-field measurements (a shutter at the back of the module allows to open/close this central hole) [9]

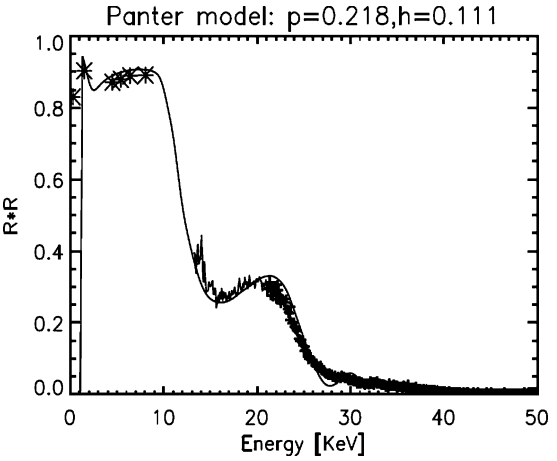

Fig. 5 Reflectivity R(parabola) $\times$ R(hyperbola) as function of energy for a W/Si multilayer shell. The solid line represents a model fit (with incidence angles of 0.218° and 0.111°, respectively), high-energy data points ($E > 10$ keV) with EPIC-pn CCD camera and continuum source, low-energy data points ($E < 10$ keV) using PSPC and target source at PANTER [9]

vignetting effects a net reduction in *measured* effective area is obtained [6]. With longer focal length and higher energy the effects of a divergent beam become more important. Moreover, the finite distance of the source from the mirror entrance causes also enhanced single reflections, i.e. photons are reflected at the paraboloid but do not hit the hyperboloid anymore and thus do not reach the focal point. These effects, however, can be calculated and taken into account when analysing the calibration data [8].

Figure 4 shows a NiCo replicated shell with W/Si multilayer coating (MSFC+SAO) mounted on a spider, just at the entry of the PANTER vacuum tube to the instrument chamber. The shell was 150 μm thick, 23 cm in diameter, and 42.6 cm long, with a focal length $f =$ 10 m (which required this location for the measurements). The optics area (after subtraction of single reflections and spider rib obstruction) was 2.69 cm^2 [9]. The half-energy width (HEW) of the point spread function was 26.5–30.5 arcsec for energies in the 0.27–8.04 keV range. At higher energies the HEW determination was affected by pile-up, because of the good performance of the mirror in terms of HEW and effective area. By de-focusing the beam the photons were spread out over a larger CCD area and pile-up effects could be reduced, and the total reflectivity could accurately be measured. This is shown in Figure 5. The solid line represents a model for incidence angles of 0.218° and 0.111° at parabola and hyperbola, respectively. Low-energy data have been taken with the *ROSAT* PSPC and the target source while the high-energy data points were obtained with the *XMM-Newton* EPIC-pn CCD camera and a continuum source (up to 50 keV).

A different multilayer (Pt/C) coated Ni shell produced by INAF-OAB was calibrated at PANTER in a similar manner (the mirror shell was integrated and installed onto a jig which was put into the vacuum tube). The HEW was measured to be 39.4–53.8 arcsec in the 0.27–8.04 keV range, and 65.1 arcsec at 25 keV. The measured and modelled two-reflection reflectivities for this shell are displayed in Figure 6 [8].

4 Summary and conclusions

We have shown that the PANTER X-ray Test Facility is not only well-suited for the calibration and characterisation of short focal length X-ray mirror performance parameters like effective

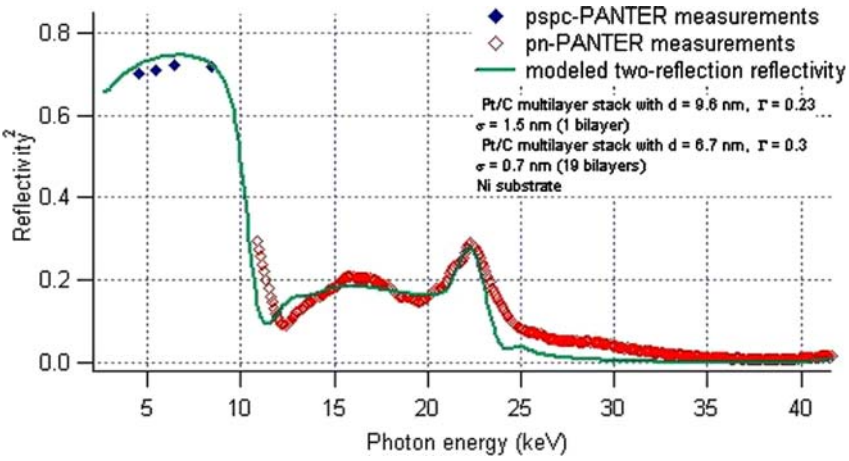

Fig. 6 Reflectivity R(parabola) $\times$ R(hyperbola) as function of energy for a Pt/C multilayer shell, with model (solid line) for incidence angles of 0.257° and 0.129°, respectively [8]

area and half-energy width in the "classical" soft X-ray range (up to 15 keV). It can very well also be used for longer focal lengths (here: 10 m) where the mirror sample will be put into the vacuum tube. Moreover, the *XMM-Newton* EPIC-pn CCD camera with the considerable quantum efficiency at energies as high as 50 keV combined with a high-flux X-ray source allow the measurement of mirror shells at hard X-rays. Examples of such calibrations were multilayer coated nickel shells (W/Si, Pt/C). We are planning a further growth of the equipment at the PANTER facility and significant improvements are projected in terms of spatial and spectral resolution of the focal plane instrumentation (as well as higher quantum efficiencies) up to 50 keV.

Acknowledgements We would like to thank Bernd Aschenbach for critical reading and useful comments.

References

1. Giacconi, R., Gursky, H., Paolini, F.R., Rossi, B.B.: Evidence for X-rays from sources outside the solar system. Phys. Rev. Lett. **9**, 439–443 (1962)
2. Aschenbach, B.: Design, construction, and performance of the Rosat high-resolution X-ray mirror assembly. Appl. Opt. **27**, 1404–1413 (1988)
3. Aschenbach, B.: X-ray telescopes. Rep. Prog. Phys. **48**, 579–629 (1985)
4. Ramsey, B.D., Austin, R.A., Decher, R.: Instrumentation for X-Ray Astronomy. Space Sci. Rev. **69**, 139–204 (1994)
5. Wolter, H.: Spiegelsysteme streifenden Einfalls als abbildende Optiken für Röntgenstrahlen. Annalen der Physik, **10**, 94–114 (1952)
6. VanSpeybroeck, L.P. Chase, R.C.: Design Parameters of Paraboloid-Hyperboloid Telescopes for X-ray Astronomy. Appl. Opt. **11**, 440–445 (1972)
7. Aschenbach, B., Briel, U.G., Haberl, F., Bräuninger, H., Burkert, W., Oppitz, A., Gondoin, P., Lumb, D.H.: Imaging performance of the XMM-Newton x-ray telescopes. Proc. SPIE, **4012**, 731–739 (2000)
8. Pareschi, G., Basso, S., Citterio, O., Ghigo, M., Mazzoleni, F., Spiga, D., Burkert, W., Freyberg, M.J., Hartner, G.D., Conti, G., Mattaini, E., Grisoni, G., Valsecchi, G., Negri, B., Parodi, G., Marzorati, A., dell'Acqua, P.: Development of grazing-incidence multilayer mirrors by direct Ni electroforming replication: a status report. Proc. SPIE, **5900**, 47–58 (2005)

9. Romaine, S.E., Pareschi, G., Gorenstein, P., Bruni, R.J., Basso, S., Citterio, O., Ghigo, M., Mazzoleni, F., Conti, G., Ramsey, B.D., Speegle, C., O'Dell, S.L., Gubarev, M.V., Engelhaupt, D.E., Burkert, W., Hartner, G.D., Freyberg, M.J.: Development of a prototype nickel optic for the Constellation-X hard-x-ray telescope: part III. Proc. SPIE, **5900**, 225–231 (2005)
10. Bräuninger, H., Burkert, W., Hartner, G.D., Citterio, O., Ghigo, M., Mazzoleni, F., Pareschi, G., Spiga, D.: Calibration of hard X-ray (15–50 keV) optics at the MPE test facility PANTER. Proc. SPIE, **5168**, 283–293 (2004)
11. Pfeffermann, E., Briel, U.G., Hippmann, H., Kettenring, G., Metzner, G., Predehl, P., Reger, G., Stephan, K.H., Zombeck, M., Chappell, J., Murray, S.S.: The focal plane instrumentation of the ROSAT Telescope. Proc. SPIE, **733**, 519–532 (1986)
12. Pfeffermann, E., Briel, U.G., Freyberg, M.J.: Design and in-orbit-performance of the position sensitive proportional counter onboard the X-ray astronomy satellite ROSAT. Nucl. Inst. Meth. Phys. Res. A, **515**, 65–69 (2003)
13. Strüder, L., Briel, U.G., Dennerl, K., Hartmann, R., Kendziorra, E., Meidinger, N., Pfeffermann, E., Reppin, C., Aschenbach, B., Bornemann, W., Bräuninger, H., Burkert, W., Elender, M., Freyberg, M.J., Haberl, F., Hartner, G.D., Heuschmann, F., Hippmann, H., Kastelic, E., Kemmer, S., Kettenring, G., Kink, W., Krause, N., Müller, S., Oppitz, A., Pietsch, W., Popp, M., Predehl, P., Read, A., Stephan, K.-H., Stötter, D., Trümper, J., Holl, P., Kemmer, J., Soltau, H., Stötter, R., Weber, U., Weichert, U., von Zanthier, C., Carathanassis, D., Lutz, G., Richter, R.H., Solc, P., Böttcher, H., Kuster, M., Staubert, R., Abbey, A., Holland, A., Turner, M., Balasini, M., Bignami, G.F., La Palombara, N., Villa, G., Buttler, W., Gianini, F., Lainé, D., Lumb, R., Dhez, P.: The European Photon Imaging Camera on XMM-Newton: The pn-CCD camera. Astron. Astroph. **365**, L18–L26 (2001)
14. Meidinger, N., Bonerz, S., Eckhardt, R., Englhauser, J., Hartmann, R., Hasinger, G., Holl, P., Krause, N., Lutz, G., Richter, R., Soltau, H., Strüder, L., Trümper, J.: First measurements with a frame store PN-CCD X-ray detector. Nucl. Inst. Meth. Phys. Res. A, **512**, 341–349 (2003)
15. Predehl, P., Friedrich, P., Hasinger, G., Pietsch, W.: ROSITA. Astron. Nachr. **324**, 128–131 (2003)
16. Parmar, A.N., Arnaud, M., Barcons, X., Bleeker, J.M., Hasinger, G., Inoue, H., Palumbo, G., Turner, M.J.L.: Science with XEUS: the X-Ray Evolving Universe Spectroscopy mission. Proc. SPIE, **5488**, 388–393 (2004)